



HAL
open science

Contribution to the modelling of a Low Temperature PEM Fuel Cell in aeronautical conditions

Alexandra Pessot, Christophe Turpin, Amine Jaafar, Guillaume Gager, Julien D'arbigny

► **To cite this version:**

Alexandra Pessot, Christophe Turpin, Amine Jaafar, Guillaume Gager, Julien D'arbigny. Contribution to the modelling of a Low Temperature PEM Fuel Cell in aeronautical conditions. 12th International Conference on Modeling and Simulation of Electric Machines, Converters and Systems (ELECTRIMACS), Jul 2017, Toulouse, France. hal-04850768

HAL Id: hal-04850768

<https://hal.science/hal-04850768v1>

Submitted on 20 Dec 2024

HAL is a multi-disciplinary open access archive for the deposit and dissemination of scientific research documents, whether they are published or not. The documents may come from teaching and research institutions in France or abroad, or from public or private research centers.

L'archive ouverte pluridisciplinaire **HAL**, est destinée au dépôt et à la diffusion de documents scientifiques de niveau recherche, publiés ou non, émanant des établissements d'enseignement et de recherche français ou étrangers, des laboratoires publics ou privés.

CONTRIBUTION TO THE MODELLING OF A LOW TEMPERATURE PEM FUEL CELL IN AERONAUTICAL CONDITIONS

Alexandra Pessot^{1,2}, Christophe Turpin², Amine Jaafar², Guillaume Gager¹, Julien d'Arbigny³

1. Institute of Technology Antoine de Saint Exupéry (IRT Saint Exupéry), More Electrical Aircraft department, F-31432 Toulouse, France
2. LAPLACE, University of Toulouse, CNRS, INPT, UPS, F-31071 Toulouse, France
3. ZODIAC AEROTECHNICS, F-78373 Plaisir, France

e-mail: alexandra.pessot@irt-saintexupery.com

Abstract – In recent work carried out in the LAPLACE laboratory, a model of PEM fuel cells in variable operating conditions was proposed and investigated [1] [2]. This model allows predicting with satisfactory results the polarization curves of PEM single cells which operate in a defined operating range. First results seem also promising if we want to extend the validity domain of this model to other operating condition ranges. The purpose of our work is to study the behaviour of this model when it is applied to a PEM fuel cell stack operating in typical aeronautical conditions in order to be able to estimate its performance. Particular attention will be paid to low pressure functioning. An experimental database is created using the Design of Experiments method and is then exploited to parametrize the model. First modelling results will be presented and analysed.

Keywords – PEM fuel cell, aeronautical application, Design of Experiments, modelling.

1. INTRODUCTION

Nowadays, fuel cells are getting an increasing amount of interest from the actors of the aeronautical industry and their integration in airplanes is considered as a consistent solution [1] [2]. However, even if this technology is quite mature in automotive and stationary sectors, there are still many questions about how the operating conditions specific to aeronautical environment will influence the functioning and the performance of fuel cells [3].

In the thesis work of Isabelle Labach carried out recently in the LAPLACE laboratory, a model of H₂/Air PEM fuel cells in variable operating conditions was proposed [4]. This model was validated with single cells. Impacting factors which were considered are temperature, pressure, air relative humidity and air stoichiometry. The proposed model was parameterized thanks to a database created with Design of Experiments method. Experimental relations were then established to express the variation of the model parameters as a function of the operating conditions. This model allowed predicting with satisfactory results the polarization curves of PEM single cells which operate in a given range of

operating conditions. In addition, results seem also promising to estimate polarization curves of cells operating outside the defined range.

Zodiac Aerotechnics develops and produces PEM fuel cell systems which are dedicated to aeronautical applications. A benchmark study has been achieved in order to compare performances of several stacks supplied by Zodiac Aerotechnics. Tests include a study of the performance of the stacks submitted to operating conditions specific to aeronautical applications like low temperatures and low pressures.

The idea proposed in this article is to use this test campaign to provide first elements to model PEM fuel cell in aeronautical conditions. The first part of our work is to apply the previous developed model to stacks supplied by a different company (compared to the previous work [4]) and submitted to another operating field. Additional work consists then in studying the behavior of the model for operating conditions specific to aeronautical environment.

2. EXPERIMENTAL APPROACH

2.1. TEST BENCH DESCRIPTION

One test bench is dedicated to the Benchmark testing. The test bench is equipped with 2 commercial pumps, one for hydrogen and one for oxygen, in order to be able to recreate subatmospheric pressure functioning.

Stacks which are used in the Benchmark study are provided by Zodiac Aerotechnics.

2.2. DESIGN OF EXPERIMENTS (DOE)

Tests are organized following the Design of Experiments approach. The first DoE (DoE n°1) is constructed with a factorial plan made of 4 factors: temperature T , pressure P , air relative humidity RH_{air} and hydrogen relative humidity RH_{H_2} .

I. Factors and associated levels for DoE n°1

Factor	Levels
T	65 – 80 °C
P	0.8 – 1 – 1.3 – 1.5 bars
RH_{air}	30 – 50 %
RH_{H_2}	30 – 50 %

Air and hydrogen stoichiometries are held constants: $\lambda_{air} = 2$ and $\lambda_{hyd} = 1.5$.

In all, 32 points, defined by their operation condition set (T , P , RH_{air} , RH_{H_2}), have to be tested in the DoE n°1.

The second part of the tests (DoE n°2) is entirely devoted to the study of operating conditions specific to aeronautical environment. DoE contains points at low pressures until 0.6 bar and at low temperatures until 40 °C.

2.3. EXPERIMENTAL PROCEDURE DESCRIPTION

For each point of the achieved DoE, a polarization curve is plotted (18 levels). Electrochemical Impedance Spectroscopy (EIS) measures are carried out from 16 kHz to 1 Hz at each current level. A reference polarization curve is plotted at the beginning and at the end of each testing day in order to verify the stability of the fuel cell.

2.4. FIRST EXPERIMENTAL RESULTS

First experimental results for DoE n°1 applied to the stack n°1 are given in Figure 2. Polarization curves are plotted for every operating condition set.

It appears that best performances for this stack are obtained for $T = 65^\circ\text{C}$, $P = 1.5$ bar, $RH_{air} = 50\%$ and $RH_{H_2} = 50\%$.

In contrast, a decline of the performances is observed for the functioning at low pressures, especially for $P = 0.8$ bar. Curve n°28, which correspond to the operating conditions $T = 80^\circ\text{C}$, $P = 0.8$ bar, $RH_{air} = 30\%$ and $RH_{H_2} = 30\%$, could not have been plotted because cell voltages were too lows (security cell voltage level was reached). These first observations are in accordance with available literature elements showing performances drop with the pressure decrease [5] [6] [7].

3. PEM FUEL CELL MODEL

3.1. PREVIOUS MODELING WORK

The global model equation is:

$$U_{FC} = E_{rev} - \eta_{act} - \eta_{diff} - \eta_{ohm} \quad (1)$$

with

U_{FC} : Fuel Cell voltage

E_{rev} : theoretical thermodynamic reversible voltage

η_{act} , η_{diff} , η_{ohm} : activation, diffusion and ohmic losses

The thermodynamic reversible voltage can be defined thanks to the following relation:

$$E_{rev} = E_{rev}^\circ - \frac{RT}{nF} \ln \left[p_{H_2} \left(p_{O_2}^{0.5} \right) \right] \quad (2)$$

Activation losses, represented by η_{act} , are linked to the chemical reactions kinetics. Thanks to a simplified Butler-Volmer equation, η_{act} can be written:

$$\eta_{act} = \frac{RT}{\alpha n F} \ln \left(\frac{J + J_n}{J_0} \right) \quad (3)$$

Diffusion losses η_{diff} refer to the reactant gas transport in the Gas Diffusion Layer (GDL) and in the Active Layer (AL). These losses are mainly occurring at the cathode side. Combining Fick and Faraday laws, and assuming that diffusion losses are mainly occurring at the cathode side, the following relation can be proposed for η_{diff} :

$$\eta_{diff} = \left| \frac{RT}{\beta n F} \ln \left(1 - \frac{J}{J_{lim}} \right) \right| \quad (4)$$

Ohmic losses η_{ohm} includes voltage drops linked to the membrane resistance, to the electronic resistance of the others elements of the cell (electrodes, bipolar plates, etc.) and to contact resistances existing between the different layers.

Assuming that the main ohmic losses are located in the membrane, η_{ohm} can be expressed by:

$$\eta_{ohm} = R_{ohm}J \text{ with } R_{ohm} = R_{memb} \quad (5)$$

II. Equation parameters

Symbol	Quantity
α	charge transfer coefficient
n	number of exchanged electrons in the global reaction ($n = 2$)
J_n	parasitic reaction equivalent current density (A/cm ²)
J_0	exchange current density (A/cm ²)
β	diffusion coefficient
J_{lim}	limiting diffusion current density (A/cm ²)
R_{ohm}	ohmic resistance ($\Omega \cdot \text{cm}^2$)
R_{memb}	membrane resistance ($\Omega \cdot \text{cm}^2$)

Fuel cell voltage can be expressed with the following relation:

$$U_{FC} = E_{rev} - \frac{RT}{\alpha n F} \ln\left(\frac{J + J_n}{J_0}\right) - \left[\frac{RT}{\beta n F} \ln\left(1 - \frac{J}{J_{lim}}\right)\right] - R_{ohm}J \quad (6)$$

Parameters to be identified are a priori α , J_0 , J_n , β and J_{lim} .

R_{ohm} is not identified but measured thanks to EIS. As described before, R_{ohm} is assimilated to R_{memb} which is given by the intersection of the spectrum with the abscissa axis.

In recent work of the laboratory, a quasi-static model taking into account the dependency on operating conditions was proposed. The influence of temperature T , pressure P , air relative humidity RH_{air} and air stoichiometry λ_{air} on the polarization curve is studied and modelled. A DoE using 4 factors (T , P , RH_{air} , λ_{air}) with 2 levels was performed to make an experimental data base (16 polarization curves and EIS measures). Thanks to first experimental results, but also to bibliographical work, the precedent model was completed to integrate the operating condition influences:

$$U_{FC} = E_{rev}(T, P) - \frac{RT}{\alpha n F} \ln\left(\frac{J + J_n(T, P)}{J_0(T, P)}\right) - \left[\frac{RT}{\beta n F} \ln\left(1 - \frac{J}{J_{lim}(T, P, RH_{air}, \lambda_{air})}\right)\right] - R_{ohm}(T, P, RH_{air}, \lambda_{air})J \quad (7)$$

α is considered invariant with the operating conditions: $\alpha = 0.5$.

β , which is related to electrode geometric properties, is also considered invariant with the operating conditions but has to be determined.

Parameters to be identified for each set (T , P , RH_{air} , λ_{air}) are J_0 , J_n , β and J_{lim} . The approach proposed is to carry out a simultaneous optimization on all the polarization curves. A least square criteria is used for optimization process.

In the second part of this modelling work, relations giving the variation of the model parameters as a function of operating conditions were developed. Combine effects of several operating factors could also be taken into account with the introduction of interconnected factors in these laws.

The relation giving the exchange current as a function of operating conditions is a physical based relation constructed with an Arrhenius law.

$$J_0(T, P) = J_{0_arr} \left(\frac{P}{P_{ref}}\right)^\gamma \exp\left(-\frac{E_{act}}{RT} \left(1 - \frac{T}{T_{ref}}\right)\right) \quad (8)$$

with J_{0_arr} reference exchange current density, γ reaction order with respect to oxygen and E_{act} activation energy.

$$J_n(T, P) = J_{n_mean} + a_{Jn} \times t + b_{Jn} \times p + c_{Jn} \times t \times p \quad (9)$$

with J_{n_mean} , a_{Jn} , b_{Jn} , c_{Jn} : constants to be identified thanks to the experimental data.

Relations for the limiting current is giving in Eq. 10 with J_{lim_mean} , a_{Jlim} , b_{Jlim} , c_{Jlim} , d_{Jlim} , e_{Jlim} , f_{Jlim} , g_{Jlim} , h_{Jlim} , i_{Jlim} and j_{Jlim} constants to be identified thanks to the experimental data.

A unique set of parameters is obtained for all the curves.

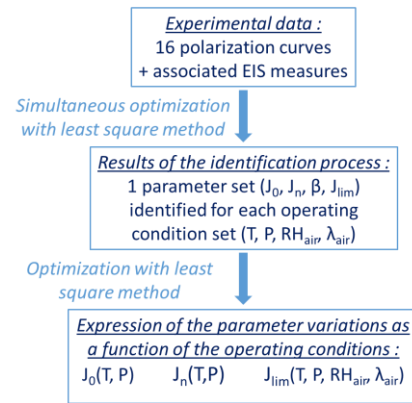


Fig. 1. Illustration of the modelling approach

Last step of the modelling approach was the validation of the model with points which are not considered in the DoE testing or with points taken outside the defined operating field. Quite satisfactory results were obtained.

3.2. VALIDATION OF THE MODELING TOOL

The aim of this step is to validate our modeling tool before applying it to our experimental database.

A set of parameter is arbitrarily chosen to be the reference parameter set. Using these parameters, a “fictional” database is created applying laws and relations which compose the studied model. This database is the equivalent of the experimental database in a classical optimization process. The optimization process is then applied to our fictional database to identify a parameter set using a least square criteria. At the end, these estimated parameters are compared to the reference parameters, which are known because database has been defined with imposed reference, in order to validate the identification tool.

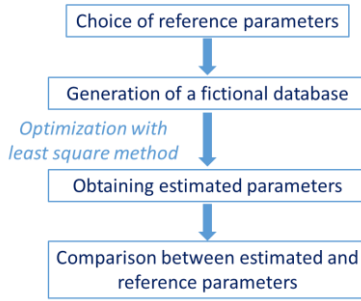


Fig. 2. Illustration of the validation step of the identification tool

This method has been applied using the parameters identified for the DoE defined in the work of I. Labach [4]. It is to say that 16 operating condition sets have been considered (see table III).

III. Factors and associated levels for DoE n°1

Factor	Levels
T	60 – 75 °C
P	1.5 – 4 bars
RH_{air}	70 – 90 %
λ_{air}	1.5 - 2.25

Identification of J_0 , J_n , β and J_{lim}

A database giving several polarization curves (voltage U_{cell} versus current density) for different operating conditions is created using imposed reference parameters.

Parameters to be identified are J_0 , J_n , β and J_{lim} . As in the thesis work of I. Labach [4], parameter dependencies on operating conditions are considered.

IV. Parameter dependencies on operating conditions

Parameter	Dependencies on operating conditions
J_0	T, P
J_n	T, P
β	$\beta = \text{constant}$
J_{lim}	$T, P, RH_{air}, \lambda_{air}$

For example, J_0 depends on T and P . As 4 different couples (T, P) are considered to create the fictional experimental database, 4 J_0 have to be identified.

The global parameter vector to be identified is (see Fig.3. for more details):

$$\left[J_{01}, J_{02}, J_{03}, J_{04}, J_{n1}, J_{n2}, J_{n3}, J_{n4}, \beta, J_{lim1}, \dots, J_{lim16} \right]$$

Every set of operating conditions is linked to a couple of parameters $(J_0, J_n, \beta, J_{lim})$.

Curve number	t	p	rh_{air}	λ_{air}	J_0	J_n	β	J_{lim}
1	1	1	1	1	J_{01}	J_{n1}	β	J_{lim1}
2	1	1	1	-1	J_{01}	J_{n1}	β	J_{lim2}
3	1	1	-1	1	J_{01}	J_{n1}	β	J_{lim3}
4	1	1	-1	-1	J_{01}	J_{n1}	β	J_{lim4}
5	1	-1	1	1	J_{02}	J_{n2}	β	J_{lim5}
6	1	-1	1	-1	J_{02}	J_{n2}	β	J_{lim6}
7	1	-1	-1	1	J_{02}	J_{n2}	β	J_{lim7}
8	1	-1	-1	-1	J_{02}	J_{n2}	β	J_{lim8}
9	-1	1	1	1	J_{03}	J_{n3}	β	J_{lim9}
10	-1	-1	1	1	J_{04}	J_{n4}	β	J_{lim10}
11	-1	-1	-1	1	J_{04}	J_{n4}	β	J_{lim11}
12	-1	-1	1	-1	J_{04}	J_{n4}	β	J_{lim12}
13	-1	1	-1	1	J_{03}	J_{n3}	β	J_{lim13}
14	-1	1	1	-1	J_{03}	J_{n3}	β	J_{lim14}
15	-1	1	-1	-1	J_{03}	J_{n3}	β	J_{lim15}
16	-1	-1	-1	-1	J_{04}	J_{n4}	β	J_{lim16}

Fig. 3. Link between operating condition set and associated parameter set $(J_0, J_n, \beta, J_{lim})$

In this table, variables t , p , rh_{air} and λ_{air} are normalized compared to the middle point of the DoE. For example, t is given by:

$$t = \frac{T - T_{moy}}{T_{norm}} \quad (10)$$

$$\text{with } T_{moy} = \frac{T_{max} + T_{min}}{2} \quad \text{and} \quad T_{norm} = \frac{T_{max} - T_{min}}{2}$$

The algorithm objective is to minimize the error ε using a least square criteria (Eq. 11).

$$\varepsilon = \sum_{n_curves} \sum_j \left(\frac{U_{cell_estimated}(j) - U_{cell_reference}(j)}{U_{cell_reference}(j)} \right)^2$$

Parameter	Reference parameter	Estimated parameter	Relative error
J_{o1}	$3.91 \times 10^{-6} \text{ A/cm}^2$	$3.91 \times 10^{-6} \text{ A/cm}^2$	$8,73 \times 10^{-9}$
J_{o2}	$2.44 \times 10^{-6} \text{ A/cm}^2$	$2.44 \times 10^{-6} \text{ A/cm}^2$	$5,72 \times 10^{-8}$
J_{o3}	$1.59 \times 10^{-6} \text{ A/cm}^2$	$1.59 \times 10^{-6} \text{ A/cm}^2$	$1,66 \times 10^{-8}$
J_{o4}	$9.76 \times 10^{-7} \text{ A/cm}^2$	$9.76 \times 10^{-7} \text{ A/cm}^2$	$1,95 \times 10^{-8}$
J_{n1}	0.006 A/cm^2	0.006 A/cm^2	$6,53 \times 10^{-9}$
J_{n2}	0.002 A/cm^2	0.002 A/cm^2	$1,12 \times 10^{-8}$
J_{n3}	0.005 A/cm^2	0.005 A/cm^2	$1,88 \times 10^{-7}$
J_{n4}	0.001 A/cm^2	0.001 A/cm^2	$6,20 \times 10^{-8}$
β	0.122	0.122	$1,63 \times 10^{-10}$
J_{lim1}	1.85 A/cm^2	1.85 A/cm^2	$6,17 \times 10^{-9}$
J_{lim2}	1.54 A/cm^2	1.54 A/cm^2	$1,42 \times 10^{-8}$
J_{lim3}	2.11 A/cm^2	2.11 A/cm^2	$1,90 \times 10^{-8}$
J_{lim4}	1.58 A/cm^2	1.58 A/cm^2	$8,66 \times 10^{-9}$
J_{lim5}	1.23 A/cm^2	1.23 A/cm^2	$7,59 \times 10^{-9}$
J_{lim6}	1.10 A/cm^2	1.10 A/cm^2	$5,78 \times 10^{-10}$
J_{lim7}	1.39 A/cm^2	1.39 A/cm^2	$1,58 \times 10^{-8}$
J_{lim8}	1.15 A/cm^2	1.15 A/cm^2	$3,35 \times 10^{-10}$
J_{lim9}	1.37 A/cm^2	1.37 A/cm^2	$8,91 \times 10^{-9}$
J_{lim10}	1.12 A/cm^2	1.12 A/cm^2	$6,80 \times 10^{-10}$
J_{lim11}	1.14 A/cm^2	1.14 A/cm^2	$8,24 \times 10^{-10}$
J_{lim12}	1.04 A/cm^2	1.04 A/cm^2	$1,44 \times 10^{-9}$
J_{lim13}	1.58 A/cm^2	1.58 A/cm^2	$6,68 \times 10^{-9}$
J_{lim14}	1.23 A/cm^2	1.23 A/cm^2	$8,43 \times 10^{-9}$
J_{lim15}	1.33 A/cm^2	1.33 A/cm^2	$1,51 \times 10^{-9}$
J_{lim16}	1.04 A/cm^2	1.04 A/cm^2	$1,38 \times 10^{-10}$

Fig. 3. Identification results for the parameter vector

Results show a maximal relative error lower than 10^{-7} .

Identification of the parameters for the variation laws giving J_0 , J_n , β and J_{lim} as a function of operating conditions

Once the vector containing 25 parameters has been found, the objective is to determine the general variation laws of J_0 , J_n and J_{lim} as a function of operating conditions T , P , RH_{air} and λ_{air} .

Parameter vectors which have to be identified are presented below:

$$\begin{bmatrix} J_{0_arr} \\ \gamma \\ E_{act} \end{bmatrix} \quad \begin{bmatrix} J_{n_moy} \\ a_{Jn} \\ b_{Jn} \\ c_{Jn} \end{bmatrix} \quad \begin{bmatrix} J_{lim_mean} \\ a_{Jlim} \\ b_{Jlim} \\ c_{Jlim} \\ d_{Jlim} \\ e_{Jlim} \\ f_{Jlim} \\ g_{Jlim} \\ h_{Jlim} \\ i_{Jlim} \\ j_{Jlim} \end{bmatrix}$$

As for the previous optimization process, the algorithm objective is to minimize the error using a least square criteria.

Parameter	Reference parameter	Estimated parameter	Relative error
J_{0_arr}	$9.70 \times 10^{-7} \text{ A/cm}^2$	$9.70 \times 10^{-7} \text{ A/cm}^2$	0.1577×10^{-8}
γ	0.5	0.5	0.3421×10^{-8}
E_{act}	$58.8 \times 10^3 \text{ J/mol}$	$58.8 \times 10^3 \text{ J/mol}$	0.0580×10^{-8}

Fig. 4. Identification results for $J_0(T, P)$

Parameter	Reference parameter	Estimated parameter	Relative error
J_{n_mean}	0.0034 A/cm^2	0.0034 A/cm^2	0.0123×10^{-7}
a_{Jn}	3.2×10^{-4}	3.2×10^{-4}	0.2450×10^{-7}
b_{Jn}	0.0018	0.0018	0.0113×10^{-7}
c_{Jn}	1.6×10^{-4}	1.6×10^{-4}	0.2661×10^{-7}

Fig. 5. Identification results for $J_n(T, P)$

Parameter	Reference parameter	Estimated parameter	Relative error
J_{lim_mean}	1.3620	1.3620	0.0023×10^{-6}
a_{Jlim}	0.1310	0.1310	0.0121×10^{-6}
b_{Jlim}	0.2096	0.2096	0.0098×10^{-6}
c_{Jlim}	-0.0542	-0.0542	0.0340×10^{-6}
d_{Jlim}	0.1070	0.1070	0.0077×10^{-6}
e_{Jlim}	0.0638	0.0638	0.0026×10^{-6}
f_{Jlim}	-0.0128	-0.0128	0.1659×10^{-6}
g_{Jlim}	0.0354	0.0354	0.0296×10^{-6}
h_{Jlim}	-0.0254	-0.0254	0.0304×10^{-6}
i_{Jlim}	0.0382	0.0382	0.0059×10^{-6}
j_{Jlim}	-0.0248	-0.0248	0.0053×10^{-6}

Fig. 6. Identification results for $J_{lim}(T, P, RH_{air}, \lambda_{air})$

Maximal error obtained between reference and estimated parameters is lower than 10^{-6} .

3.3. USE OF THIS MODEL FOR OUR DOE ANALYSIS

At present, the objective is to use the previously described model tool, which has been validated, for exploiting our real experimental database obtained with a first stack.

First difficulties to adapt the approach to our DoE testing come from several points:

- previous model and experiments were made at single cell level
- our DoE is defined with different operating factors (T , P , RH_{air} , RH_{H2}) whereas precedent DoE was made with operating factors (T , P , RH_{air} , λ_{air}).
- our DoE testing includes subatmospheric pressure tests.

Simulations are still in progress to parametrize the model.

CONCLUSION

A first step has been necessary to validate the identification tool. This tool is able to identify parameters with a satisfactory accuracy.

However, as expected, it appears that the accuracy of the optimization process is linked to the number of available curves for the identification.

The experimental database exploitation is still in progress and appears to be more difficult than expected.

ACKNOWLEDGEMENTS

The authors would like to express their sincere thanks to all the members of the FUCHYA project, the ANR and the LAPLACE laboratory.

REFERENCES

- [1] A.K. Sehra and W. Whitlow Jr., "Propulsion and power for 21 st century aviation", Progress in Aerospace Science, Vol. 40, pp. 199-235, 2004.
- [2] J.W. Pratt, L.E. Klebanoff, K. Munoz-Ramoz, A.A. Akhil, D.B. Curgus and B.L. Schenkman, Proton exchange membrane fuel cells for electrical power generation on-board commercial airplanes, Applied Energy, Vol. 101, pp. 776–796, 2013.
- [3] G. Renouard-Vallet, M. Saballus, G. Schmithals, J. Schirmer, J. Kallo and K. A. Friedrich, Improving the environmental impact of civil aircraft by fuel cell technology: concepts and technological progress, Energy & Environmental Science, pp. 1458–1468, March 2010.
- [4] I. Labach, Caractérisation et modélisation de Piles à combustible et d'Electrolyseurs PEM à conditions opératoires variables, en vue de leur association, Doctoral thesis, Institut National Polytechnique de Toulouse, France, 2016.
- [5] Q. Yan, H. Toghiani and H. Causey, Steady state and dynamic performance of proton exchange membrane fuel cells (PEMFCs) under various operating conditions and load changes, Journal of Power Sources, Vol. 161, pp. 492–502, 2006.
- [6] J. Kallo, G. Renouard-Vallet, M. Saballus, G. Schmithals, J. Schirmer and K. A. Friedrich, Fuel cell System Development and Testing for Aircraft Applications, 18th World Hydrogen Energy Conference, Proceedings, pp. 435-444, Essen, Germany, 16-21 May 2010.
- [7] T. Horde, P. Achard and R. Metkemeijer, PEMFC application for aviation: Experimental and numerical study of sensitivity to altitude, International Journal of Hydrogen Energy, Vol. 37, pp. 10818-10829, 2012.

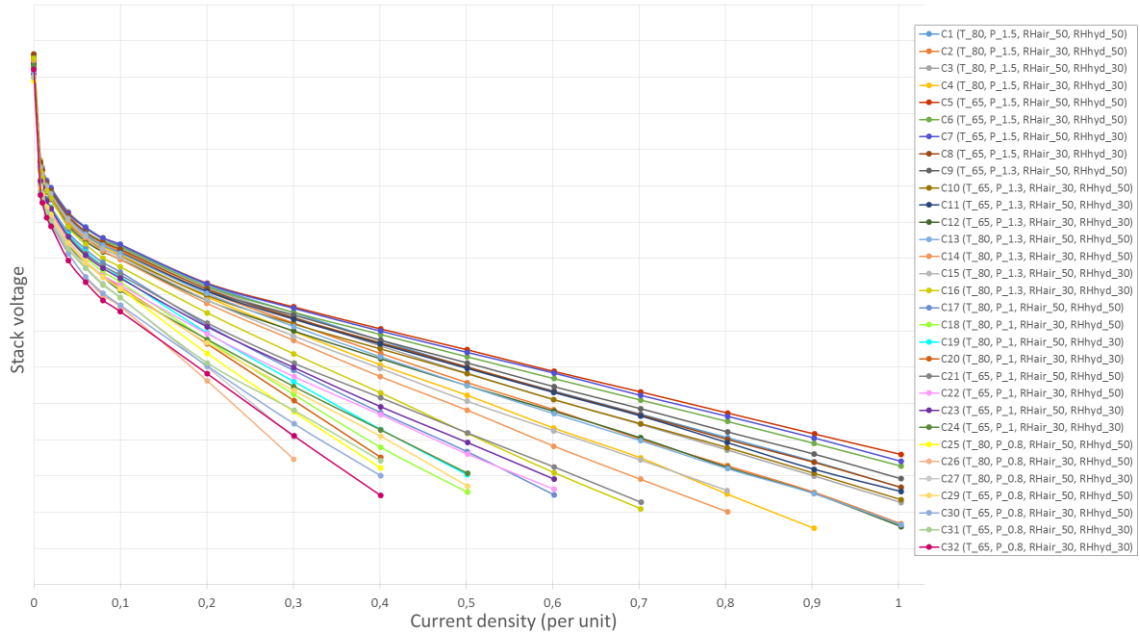


Fig. 4. Polarization curves for different operating conditions - Experimental results of the DoE n°1 for 1 stack. (*Y axis is voluntarily hidden for confidentiality reasons)

$$J_{\lim}(T, P, RH_{air}, \lambda_{air}) = J_{\lim_mean} + a_{J_{\lim}} \times t + b_{J_{\lim}} \times p + c_{J_{\lim}} \times hr + d_{J_{\lim}} \times \lambda + e_{J_{\lim}} \times t \times p + f_{J_{\lim}} \times t \times hr + g_{J_{\lim}} \times t \times \gamma + h_{J_{\lim}} \times p \times hr + i_{J_{\lim}} \times p \times \lambda + j_{J_{\lim}} \times hr \times \lambda \quad (10)$$

Eq. 10. Relation giving the limiting current density J_{\lim} as a function of operating conditions